JOURNAL OF MATERIALS SCIENCE **35** (2000) 2729–2734

Spinodal decomposition of fine-grained binary alloys: A Monte-Carlo simulation

J.-M. LIU
Laboratory of Solid State Microstructures, Nanjing University, Nanjing 210093, People's Republic of China
Institute of Materials Research and Engineering, Blk.S7, Level 3, National University of Singapore, 10 Kent Ridge Crescent, Singapore 119260; E-mail: liu-jm@imre.org.sg

L. C. LIM
Institute of Materials Research and Engineering, Blk.S7, Level 3, National University of Singapore, 10 Kent Ridge Crescent, Singapore 119260

Z. C. WU, G. H. CAO, G. CHEN, Z. G. LIU
Laboratory of Solid State Microstructures, Nanjing University, Nanjing 210093, People's Republic of China

The kinetics of spinodal decomposition of binary alloys in case of finite grain size and slow grain growth is studied by applying the Monte-Carlo method where a coupled algorithm of the spin-exchange Ising model and Q-state Potts model operates. The anisotropic energy of grain boundaries is incorporated by imposing a Potts spin lattice on the Ising crystal. We simulate the phase separation where the grain size is comparable with the spinodal length on the order of magnitude. It is revealed that the grain boundaries of low excess energy as rapid channel enhance the solute diffusion, whereas those boundaries of high excess energy hinder the solute diffusion. Depending on the system supersaturation, phase aggregation preferred at the grain boundaries is demonstrated. The spinodal kinetics is modulated by the grain growth so that the Lifshitz-Slyozov-Wagner law may no longer be applicable in spite of the scaling law roughly holds in present system.

1. Introduction

When a concentrated binary alloy is submitted to a circumstance below the spinodal line in temperature-composition phase diagram, it will finally decompose into separated two-phase structure where the solute-rich and solute-depleted phases interconnect to each other and distribute randomly. This problem represents a long time interested topic in condensed matters and materials science because it is one of the fundamental phenomena in processing many technologically important materials [1, 2]. This process is named as spinodal decomposition [3]. There are piled up a lot of publications on this topic, either on the early stage's events or the late stage's evolution. The effects of elastic strain and nonlinear fluctuations on the spinodal patterns have repeatedly been demonstrated [4–6].

It is now well known that the spinodal decomposition initiates from non-local composition fluctuations that develop irreversibly in both amplitude and wavelength. The late stage's events may incorporate strong nonlinear effects in spite of the dominant linear characters of the early stage process [3]. It bases on many reasons to pay our attention to the late stage since most materials in service exhibit the late stage's microstructure. The Cahn-Hilliard (CH) theory [7] and its improved versions (e.g. the Langer-Bar-Miller (LBM) model [8]) are no longer applicable to the late stage, whereas Monte-Carlo (MC) simulations improve significantly our understanding of the problem on the other hand [9–11]. It is established that the late stage' kinetics of decomposition (coarsening of the decomposed structure) still follows the Lifshitz-Slyozov-Wagner (LSW) law as long as the alloy exhibits short range interaction, no matter what the alloy is diluted or concentrated [11, 12]. Metallic alloys typically show short range of interaction. The other prominent character of the late stage coarsening comes to the scaling concept that all spatial-correlation properties after being scaled with the characteristic length λ of the microstructure hold unchanged with time, leaving λ the unique parameter of time dependence [12]. Here, λ may be defined as the modulating wavelength of the decomposed microstructure, which typically ranges from several nanometers to one micrometer.

Up to date, the conventional theories of spinodal decomposition deal with homogeneous systems where no high dimensional defect like grain boundary is involved [3]. Nevertheless, real materials are polycrystalline in

most cases and the grain boundaries (GBs) may impose somehow influence on the spinodal process. It is then expected that the excess boundary energy makes the GBs play as sinks of solute and attract aggregation of solute-rich phase there. If one deals with an alloy of grain size $R \gg \lambda$, i.e. coarse-grained alloy, the effect of the GBs may be negligible in spite of grain boundary precipitation and segregation may change the property of the decomposed microstructures [13]. This effect can no longer be underestimated as one deals with nano-structured materials where R becomes comparable with λ on the order of magnitude. We name this type of materials as fine-grained alloys. On the other hand, grain growth becomes a prominent sequence for the nano-sized and fine-grained materials. This introduces to the microstructure, besides λ, second characteristic length R which is also time dependent. A coupling of the two time dependent scales is then expected.

In this paper, we will study the spinodal decomposition in the concentrated fine-grained alloys by applying the MC method. Here grain size R is larger than λ but keeps the order of magnitude comparable to the latter. We assume that grain growth is a much slower sequence than phase separation. This assumption simulates the real events in most materials. We will see how kinetics and scaling of the late stage's decomposition are affected by the excess boundary energy and the slow grain growth.

We first give a brief description of our model and procedure of the MC simulation and then a detailed presentation of our simulated results. A summary is made finally.

2. Model and procedure of simulation

We start from a two-dimensional squared $L \times L$ lattice with periodic boundary conditions. Such a symmetry restricts any lattice reconstruction during the deposition. Therefore, we deal only with diffusion-dominant sequences in our simulation. The binary alloy is simulated by the spin-exchange Ising lattice where each site is occupied with either spin $S_i = 0$ for solvent A or $S_i = 1$ for solute B. The alloy composition is defined as $C_0 = N_B/(N_A + N_B)$ where N_A and N_B are the numbers of A and B in the lattice, respectively. Because $N = N_A + N_B$ keeps constant, the number of spin states of the lattice satisfies the conservation law. The conventional spin-exchange kinetics according to the Metropolis algorithm [14] is applied to simulate species diffusion in the lattice. In the lattice is also imposed at each site the second spin parameter q which represents the ordering degeneracy of the lattice, i.e. grains. We apply the Q-state Potts model [15] to simulate grain growth through migration of the GBs. Upon each site is imposed one of the Q multi-spin states ($q = 1, 2, \ldots, Q$). The Potts state of any site within one grain represents its orientation. If two nearest-neighboring sites have different Q-states, it means that they are no the GBs. The high energy state of the sites on the GBs acts as the driving force of boundary migration and then grain growth. Any site on the GBs may have its Potts spin be replaced by one of its neighbors. Those sites on the GBs show high probability of spin replacement as long as this replacement results in decaying of the system energy.

We suppose that the Ising energy between two neighboring sites with different Potts spins has no difference from that between two sites of the same Potts spin. Refer to our previous work [16], we write the Hamiltonian of the lattice, H, as:

$$\begin{aligned} H &= \sum_{\langle ij \rangle} E_{\mathrm{I}} + E_{\mathrm{P}} \\ &= -\Big[\phi_{AA} \sum_{\langle ij \rangle} (1 - S_i)(1 - S_j) + \phi_{BB} \sum_{\langle ij \rangle} S_i S_j \\ &\quad + \phi_{AB} \sum_{\langle ij \rangle} S_i(1 - S_j) + (1 - S_i) S_j \Big] \\ &\quad - J_{AA} \sum_{\langle ij \rangle} (1 - S_i)(1 - S_j)[(1 - f_{AA}) \\ &\quad + f_{AA} \delta_{\mathrm{Kr}}(\alpha, \beta)] \\ &\quad - J_{BB} \sum_{\langle ij \rangle} S_i S_j [(1 - f_{BB}) + f_{BB} \delta_{\mathrm{Kr}}(\alpha, \beta)] \\ &\quad - J_{AB} \sum_{\langle ij \rangle} [S_i(1 - S_j) + (1 - S_i) S_j][(1 - f_{AB}) \\ &\quad + f_{AB} \delta_{\mathrm{Kr}}(\alpha, \beta)] \end{aligned} \tag{1}$$

where E_{I} and E_{P} represent the Ising energy and Potts energy at site i, respectively; ϕ_{mn} $(m, n = A, B)$ denotes the Ising energy of the nearest neighbouring m-n spin-pair; $\langle ij \rangle$ represents that over nearest neighbours is summed once; $J_{mn}(\geq 0)$ is the interaction factor associated with the Potts spin-pair between the Ising spins m and n; f_{mn} is a factor to scale the Potts interaction between the Ising spins m and n, $f_{mn} = 0$ represents no Potts spin dependence of the Ising pair m-n; δ_{Kr} is the Kronecker δ function which is defined as:

$$\delta_{\mathrm{Kr}} = \frac{\lfloor 1 + (Q - 1)\, e^{-\alpha} \times e^{-\beta} \rfloor}{Q} \tag{2a}$$

where $e^{-\alpha}(\alpha = 0, 1, \ldots, Q - 1)$ are Q unit vectors pointing in the Q symmetric directions of a hypertetrahedron in $Q - 1$ dimensions. In the present simulation, however, we apply the planar Potts model instead of the standard Potts model [15] since our simulation is restricted in two-dimensional space. For the former, δ_{Kr} (we still use this symbol) should be rewritten as:

$$\delta_{\mathrm{Kr}} = \cos\left(2\pi \frac{\alpha - \beta}{Q}\right) \tag{2b}$$

In the MC simulation, we impose $\phi_{mm} = 0$ and $\phi_{AB} < 0$, indicating no interaction between the like-pair of the Ising spins but repulsive force between the unlike-pair of the Ising spins, respectively. This leads to the spinodal aggregation of the like Ising spins. We define an effective interaction factor $\phi = (\phi_{AA} + \phi_{BB})/2 - \phi_{AB} = -\phi_{AB}$. The alloy keeps homogeneous as temperature $T > T_{\mathrm{c}}$ and decomposes into two phases as $T < T_{\mathrm{c}}$ no matter with the Potts interaction, where T_{c} is the critical point of the Ising lattice defined by

TABLE I The system parameters of interaction for simulations

ϕ_{AA}	ϕ_{BB}	T/T_c	J_{mn}/kT	f_{AA}	f_{BB}	f_{AB}
0.00	0.00	2.00–0.30	1.20	1.00	0.00	0.50

$kT_c/\phi \sim 1.13$ and k is the Boltzmann constant. We also assume identical J_{mn} for all Potts spin-pairs and $J_{mn} \gg \phi_{mm} = 0$, so that the Potts sequence achieves a much lower probability than the Ising one. This yields a slow grain growth in relative to the spinodal decomposition. In order to achieve grain boundary aggregation, we take $f_{BB} = 0.0$ and $f_{AA} = 1.0$ and $f_{AB} = (f_{AA} + f_{BB})/2$. This choice permits $B-B$ pairs to stick preferably at the GBs of high excess energy rather than inside the grains.

A detailed description of the MC algorithm was presented previously [14]. The simulation is performed according to following procedure: for a given set of system parameters a lattice with random spin configuration is constructed. For a site chosen randomly, its E_I and E_P are calculated and then the probability that this site chooses either an Ising event or a Potts event is given by a partition between E_I and E_P. For an Ising event, the spin-exchange is done according to the improved Metropolis algorithm [16, 17]. The Potts spin-replacement is approved by the same algorithm. This completes a circle of simulation and then a new sequence starts. The time unit of the simulation circles is mcs. One mcs represents $L \times L$ circles completed. We simulate one system by four runs starting from different seeds of random number generation and take the average values of the simulated data for presentation.

For the present simulation, we choose $L = 128$, $Q = 24$, and $C_0 = 0.45$ at which a typical spinodal decomposition is expected. The chosen lattice is big enough to get good statistics, with the solute concentrated up to 45%. The initial grain size ranges from 15 to 50 lattice units, which is several times the maximum value of λ within the time limit reached in our simulations. The other parameters of the alloy are listed in Table I. The simulation covers from $T/T_c = 1.15$ to deep supersaturated state where $T/T_c = 0.30$. $J_{mn}/kT = 1.20$ is much bigger than $\phi_{mm} = 0.0$, predicting that the Potts event is favored with a probability of only ~1% in relative to the Ising one. Therefore, spinodal decomposition proceeds much faster than the grain growth.

3. Results of simulation

We first look at the lattice configurations at several times for $T/T_c = 0.80$, at which the maximum effect of the GBs on the decomposition is found. We simulate the homogeneous decomposition in a reference alloy where all parameters keep the same as the present alloy except that no grain boundary aggregation is preferred, i.e. $f_{AA} = f_{BB} = f_{AB} = 1.0$. The data are plotted in left column of Fig. 1 for the reference alloy and right column for the present alloy. Here the solid squared dots represent the GBs and the open circle dots for solute B, leaving the empty area for solvent A. Although the GBs in nano-materials may cover several atomic layers in thickness and fluctuate somehow, we still plot them with two lattice units in thickness.

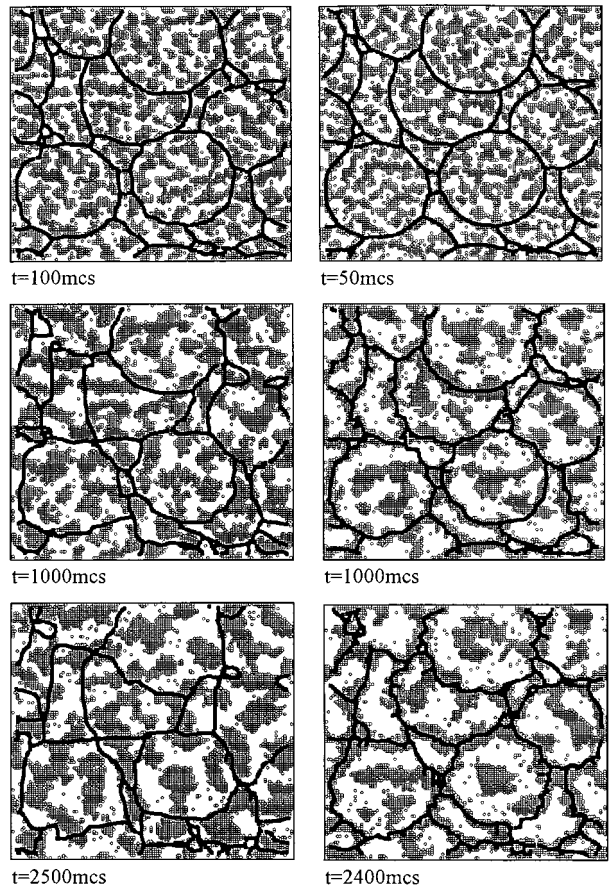

Figure 1 The grain boundary configurations and solute distributions at several times for $T/T_c = 0.80$. The left column is for the referenced alloy where $f_{mn} = 1.0$ and the right column is for present alloy.

From Fig. 1 it is clearly shown that immediately after the beginning the randomly distributed species start to aggregate into B-rich and A-rich regions. At $t = 50$ mcs, the two-phase interconnected pattern has almost been established. The early stage of spinodal decomposition develops so fast that the period after $t = 50$ mcs is covered already with coarsening of the microstructure. The phase aggregates show roughly isotropic pattern in spite of the interconnectivity. The small aggregates either shrink or stick to the neighbor big aggregates in compensation with growth of the big ones. The interconnectivity of the microstructure is enhanced through the coarsening. These show to be normal phenomena in spinodal decomposition.

In parallel to the decomposition, one also observes slow grain growth through migration of the GBs. Some small grains are swallowed by the neighboring big ones. The normal features of grain growth are shown [18].

In contrast to the left column of Fig. 1, however, significant effect of the GBs on the spinodal pattern for present alloy can be identified from the right column of Fig. 1. The decomposed structure of the present alloy achieves higher rate of coarsening than the homogeneous case. Strong grain boundary aggregation of B-rich phase is revealed. In proceeding with time, more and more B-rich aggregates inside grains shrink and

dissolve through solute diffusion toward the neighbor GBs. At $t = 2400$ mcs, one finds that the grain boundary aggregation tends to saturation. Only one to two aggregates remain inside some big grains, leaving other small grains out of aggregate. This effect leads to stripe-like shape of the B-rich phase around the GBs. Secondly, the aggregation at the GBs shows to be non-uniform. While most GBs are completely covered with B-rich stripes, some boundaries remain unoccupied or only partially occupied with solute B. This is attributed to the effect of anisotropic boundary energy that some GBs exhibit high excess energy whereas the others remain low or even close to zero. Definitely, the B-rich aggregates prefer to occupy the GBs of high excess energy. In addition, one finds that the GBs for present alloy show more irregular shape in comparison with those in the referenced alloy, whereas the GBs in the latter case are smooth and straight to some extent but also migrate more rapidly than the former case. The pinning effect of the GBs by the aggregates there is obviously responsible for these phenomena.

Furthermore, the effect of the GBs as a channel of solute diffusion is demonstrated here, no matter with the boundary aggregation preferred or not. Note here that the GBs are the most favored sites to be chosen for either Ising events or Potts sequence. We choose a scaling factor of this effect which is defined as $\sigma = N_{\mathrm{IS}}/N_{\mathrm{GB}}$, where N_{IS} is number of the chosen species (sites) which have their destination on the GBs via the Ising spin-exchange operation in one mcs and N_{GB} is the site number on the GBs. It is easily inferred that $\sigma \approx 1.0$ if no grain boundary aggregation is preferred. The data for $T/T_{\mathrm{c}} = 0.80$ are plotted in Fig. 2. At the beginning, σ achieves a value much bigger than 1.0 and then decays down to a lower value. Such a decaying can be fitted by an exponential decaying law and the underlying mechanism is the solute aggregation on the GBs. In spite of this decaying, $\sigma > 1.0$ overall time period is established, approving the GBs as a rapid channel of diffusion. However, referring to the local GBs, one identifies various individuals. Those GBs of high excess energy prefer to absorb the as many solute species as possible and finally trap them locally. At last, they play a role in hindering the solute diffusion, or in other words, they are the sinks of solutes. In contrast to this, those GBs of low and mediate excess energy becomes the rapid channels of solute diffusion. They absorb as many solutes as possible and transfer them toward the neighboring GBs of high excess energy.

Obviously, in our model one does not deal with real defect states at the GBs but approaches the defects by the high energy state. A relaxation of the excess boundary energy via the boundary aggregation damages the diffusion channel effect of the GBs. As dealing with the homogeneous spinodal sequence, we also find $\sigma \gg 1$ and its decaying becomes much slower, as shown also in Fig. 2. This gives a direct approving of the GBs' function as a rapid channel of diffusion.

On the other hand, we develop an occupation factor $\Gamma = (C_{\mathrm{GB}} - C_0)/C_{\mathrm{GB}}$ to characterize the grain boundary aggregation, where C_{GB} is the solute concentration at the GBs. Clearly, $\Gamma \approx 0.0$ if no preferred boundary aggregation performs, $\Gamma = 1 - C_0$ if all GBs are covered with the solute. We evaluate Γ as a function of T/T_{c} and time t, as plotted in Fig. 3, where T/T_{c} ranges from 2.00 to 0.30. For a fixed T/T_{c}, Γ grows rapidly from zero and then tends to be saturated. The rapid growth period covers the initial 500 mcs, indicating the boundary aggregation reaches a saturating state. At $T/T_{\mathrm{c}} = 0.80$, Γ reaches up to 0.46 after the initial growth. This value is not far from the maximum value, 0.55 for the present system, demonstrating serious boundary aggregation of the solute-rich phase.

As probing Γ as a function of T/T_{c} at any time when a saturated Γ is reached, one finds a single peaked pattern. When the peak positions at $T/T_{\mathrm{c}} = 0.80$, much lower values of Γ are evaluated at either deep or shallow supersaturation. For instance, toward the late stage $\Gamma \approx 0.15$ for $T/T_{\mathrm{c}} = 1.10$ and $\Gamma \approx 0.20$ for $T/T_{\mathrm{c}} = 0.30$. These data compromise direct evidence that the grain boundary aggregation may achieve its maximal at a moderate supersaturation. Either low

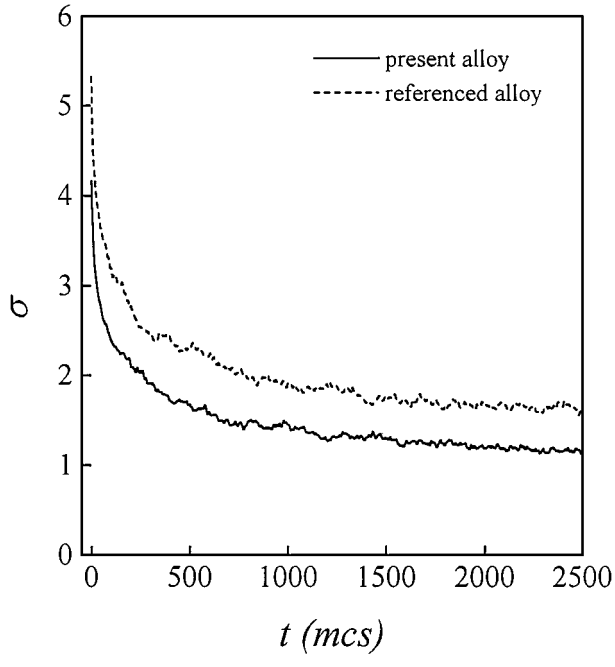

Figure 2 The scaling factor σ as a function of time for both the reference alloy and present one at $T/T_{\mathrm{c}} = 0.80$.

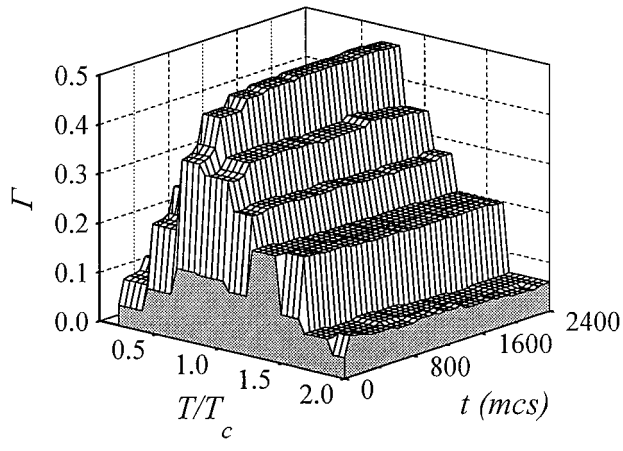

Figure 3 The occupation factor Γ as a function of T/T_{c} and t for present alloy.

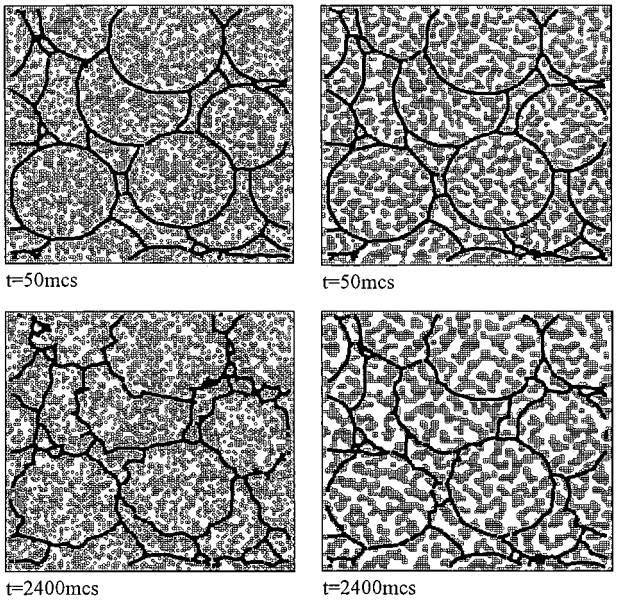

Figure 4 The grain boundary configurations and solute distributions at two times for present alloy. The left column is for $T/T_c = 1.00$ and the right one is for $T/T_c = 0.30$.

or high supersaturated alloy has its decomposed microstructure weakly affected by the GBs. For further illustration, we present in Fig. 4 the simulated lattice configurations for $T/T_c = 1.00$ (left column) and $T/T_c = 0.30$ (right column) at $t = 50$ mcs and 2400 mcs, respectively. When the decomposed alloy shows diffusive two-phase pattern at low supersaturation, a roughly uniform distributed and fine two-phase morphology is exhibited for the case of high supersaturation. It is easily understood that on one hand a low supersaturation images strong thermal fluctuations which weaken stability of the solute on the GBs, on the other hand a deep supersaturation stabilizes the fine decomposed structure.

Now let us focus on the kinetics of decomposition for $T/T_c = 0.80$. In Fig. 5a and b are plotted the evaluated spatial correlation function, $\rho(r, t)$, for the reference alloy and present one, respectively. Because the alloy is concentrated, $\rho(r)$ shows roughly regular wave-pocket pattern. The wavelength is modulated in proceeding with time through either dissolution or amplitude growth of alternative wave-pockets. Comparing Fig. 5a to b one observes strong modulation of the present system in relation to the reference one, emphasizing again the effect of the GBs on the decomposition. We choose the first zero-passing point of $\rho(r)$, R_c, as a characteristic scale of the decomposed two-phase structure and plot R_c as a function of time, as shown in Fig. 6a, where the counterpart data from the reference system are also inserted. First, it is confirmed once more that the GBs accelerates coarsening of the two-phase structure. Secondly, one fits the data according to the LSW law of following form [11, 12]:

$$R_c = R_0 + a \times t^m \tag{3}$$

where $R_0 \sim 2.0$ for $C_0 = 0.45$, a is a positive constant and m is the growth exponent. The best fitting shows $m = 0.33$, equals to the LSW exponent, for the reference

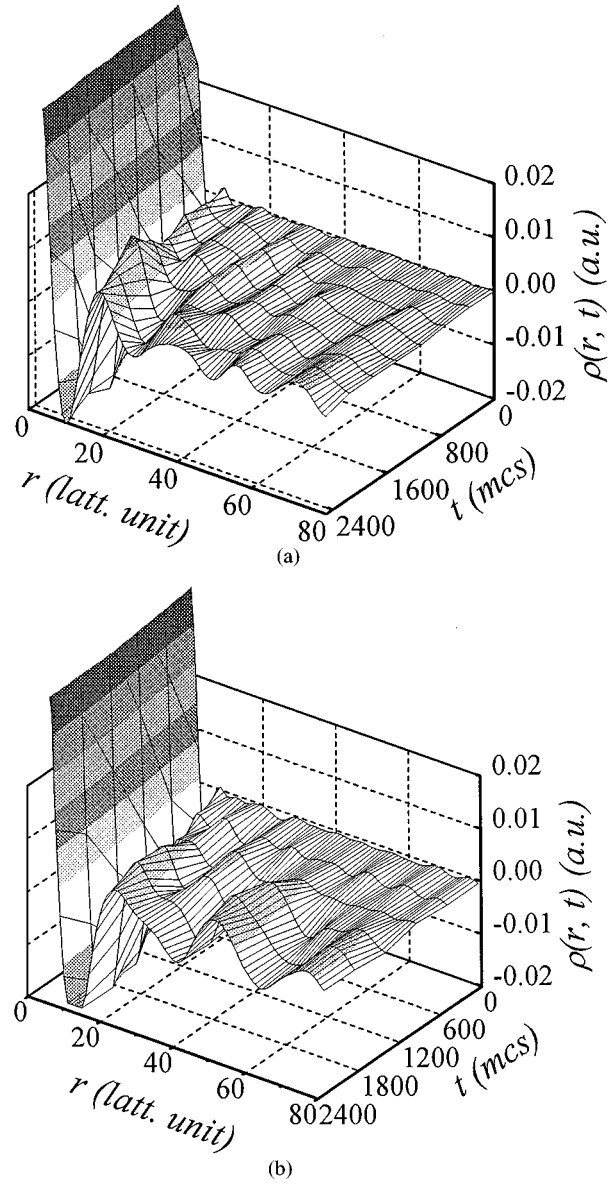

Figure 5 The spatial correlation function $\rho(r, t)$ for present alloy at $T/T_c = 0.80$.

alloy. However, for present alloy one gets $m = 0.41$, deviating from the LSW exponent. This fact reveals that the LSW scheme is no longer applicable in predicting the spinodal kinetics for the fine-grained alloys at the moderate supersaturation, in spite of this deviation may not be so big. Nevertheless, the evaluated exponent recovers back to the LSW exponent as long as the supersaturation gets to either low or high level. That the LSW law loses its validity in the present alloy is expected to result from two effects. One is the solute-rich aggregation on the GBs and secondly, there is also observed slow grain growth. Please note the fact that in Potts lattice the number of spin states are not conserved, which activates an exponent of grain growth higher than that for coarsening of the two-phase structure. We have reason to believe that grain growth in parallel to phase decomposition would definitely make exponent m higher than 1/3 as long as there exists coupling between the Ising lattice and Potts one.

Finally, we look at the scaling of correlation function $\rho(r, t)$. As shown in Fig. 6b, the curves at several times are plotted in the same diagram, subjected to scaling

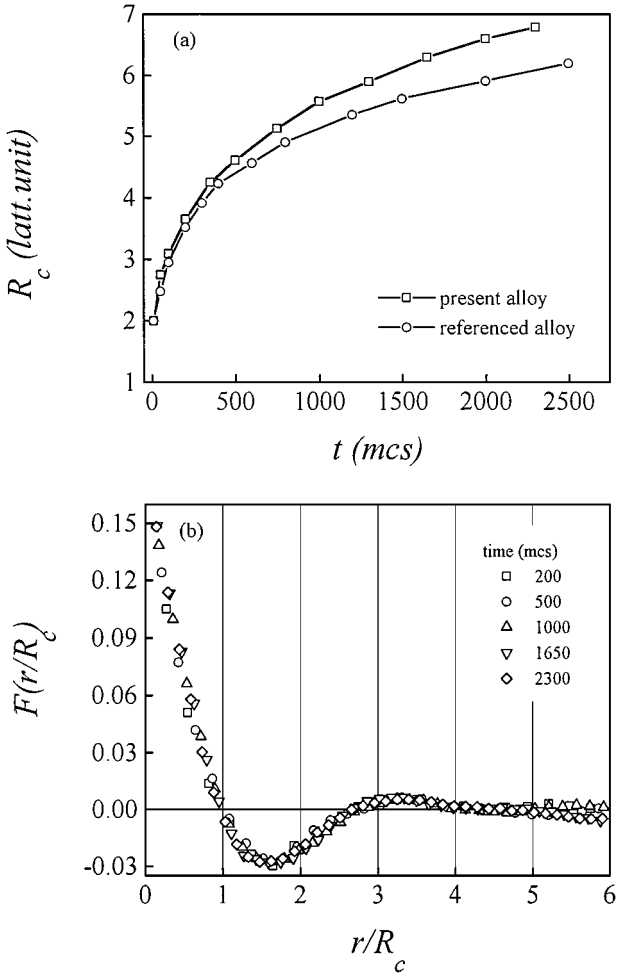

Figure 6 The characteristic scale R_c as a function of time for the referenced alloy and present one at $T/T_c = 0.80$ (a) and scaling of the data for present alloy (b).

transform $F(r/R_c) = \rho(r/R_c, t)$. It is quite clear that the curves after $t = 200$ mcs have their parts inside the third zero-crossing point fall on one specific curve within the statistical uncertainty, demonstrating the scaling law is satisfied. However, it should be noted that far away from the third zero-crossing point one observes scattering of the data. The bad statistics due to the finite lattice dimension may be responsive for the scattering.

As we reported previously, the scaling law may be broken for the diluted alloys where all solutes sink onto the GBs so that the diffusion-limited process loses its domination over to the grain-growth-controlled precipitation during the decomposition. In fact, the scaling concept reflects the self-similarity of the decomposed structure via the diffusion-limited aggregation mechanism. In contrast to this, in concentrated alloys the solute number is far over the GBs site number. Note that the system we are dealing with exhibits short range of interaction. Therefore, the solute except from those having sank onto the GBs still aggregate dominantly via the diffusion-limited steps. This seems to be the fundamental mechanism of the scaling behavior.

4. Conclusion

In conclusion, we have presented a Monte-Carlo simulation of the effect of grain boundaries on spinodal decomposition in fine-grained binary alloys where the grain size is comparable to the spinodal length. The simulated results have established the grain boundaries as the preferred channels of solute diffusion. Strong grain boundary aggregation of the solute-rich phase has been revealed through our simulation. We have demonstrated that the spinodal decomposition is accelerated by the preferred grain boundary aggregation and thus the LSW law no longer appears to be a valid description of the kinetics. The scaling property of the decomposed microstructure has been found to be held roughly.

Acknowledgement

One of the authors (JML) would like to thank the National Natural Science Foundation of China and the Key Plan for Basic Research of China for supporting this work through the special and normal project. The financial aids from the Advanced Engineering Materials program of IMRE are acknowledged.

References

1. J. D. GUNTON, M. SAM MIGUEL and P. S. SAHNI, in "Phase Transitions and Critical Phenomena, Vol. 8," edited by C. Domb and J. L. Lebowitz (Academic Press, London, 1983) p. 267.
2. K. BINDER, *Rep. Prog. Phys.* **50** (1987) 783.
3. *idem.*, in Materials Science and Technology: A Comprehensive Treatment, R.W. Cahn, P. Haasen and E. J. Kramer eds. (VCH Publishers, Weinheim, 1991) Vol. 5, p. 405.
4. J. W. CAHN and J. E. HILLIARD, *J. Chem. Phys.* **28** (1958) 258.
5. A. G. KHACHATURYAN, "Theory of Phase Transformations in Alloys," (John Wiley Publishers, New York, 1983).
6. T. MIYAZAKI, K. SEKI, M. DOI and T. KOZAKAI, *Mater. Sci. & Eng.* **77** (1986) 125.
7. J. W. CAHN, *Trans. Metall. AIME* **242** (1966) 166.
8. J. S. LANGER, M. BAR-ON and H. D. MILLER, *Phys. Rev.* **A11** (1975) 1417.
9. J. MARRO, A. B. BORTZ, M. H. KALOS and J. L. LEBOWITZ, *ibid.* **B12** (1975) 2000.
10. *Idem., ibid.* **B15** (1977) 3014.
11. D. A. HUSE, *ibid.* **B34** (1986) 7845; **B36** (1987) 5383.
12. E. T. GAWLINSKI, J. D. GUNTON and J. VINAL, *ibid.* **B39** (1989) 7266.
13. K. BINDER, in "Materials Science and Technology: A Comprehensive Treatment, Vol. 5," edited by R. W. Cahn, P. Haasen and E. J. Kramer (VCH Publishers, Weinheim, 1991) p. 305.
14. N. METROPOLIS, A. W. ROSENBLUTH, A. H. TELLER and E. TELLER, *J. Chem. Phys.* **21** (1953) 1987.
15. F. Y. WU, *Rev. Mod. Phys.* **54** (1982) 235.
16. J. M. LIU and Z. C. WU, *Scripta Mater.* **37** (1997) 385.
17. J. M. LIU and Z. G. LIU, *Mater. Lett.* **32** (1997) 67.
18. J. STAVANS, *Rep. Prog. Phys.* **56** (1993) 733.

Received 26 April
and accepted 10 December 1999